

A central role for inflammation in the pathogenesis of diabetic retinopathy

Antonia M. Joussea, ^{*,†,‡,§} Vassiliki Poulaki, ^{‡,§} Minh Ly Le, ^{*} Kan Koizumi, ^{*} Christina Esser, ^{*} Hanna Janicki, ^{*} Ulrich Schraermeyer, ^{*} Norbert Kociok, [†] Sascha Fauser, [†] Bernd Kirchhof, ^{*,†} Timothy S. Kern, ^{||} and Anthony P. Adamis, ^{‡, #}

^{*}Department of Vitreoretinal Surgery and Angiogenesis Laboratory, Center of Ophthalmology, University of Cologne, Köln, Germany; [†]Center for Molecular Medicine (ZMMK) University of Cologne, Köln, Germany; [‡]Retina Research Laboratory, Massachusetts Eye and Ear Infirmary, Harvard Medical School, Boston, Massachusetts; [§]Laboratory for Surgical Research, Children's Hospital, Harvard Medical School, Boston, Massachusetts; ^{||}Departments of Medicine and Ophthalmology and Center for Diabetes Research, Case Western Reserve University, Cleveland, Ohio; and [#]Eyeteck Research Center, Woburn, Massachusetts

Corresponding authors: Antonia M. Joussea, Department of Vitreoretinal Surgery, Center for Ophthalmology, University of Cologne, Joseph Stelzmannstr. 9, 50924 Köln, Germany. E-mail: JousseaA@aol.com; and Anthony P. Adamis, Eyeteck Research Center, 42 Cummings Park, Woburn, Massachusetts. E-mail: tony.adamis@eyetk.com

ABSTRACT

Diabetic retinopathy is a leading cause of adult vision loss and blindness. Much of the retinal damage that characterizes the disease results from retinal vascular leakage and nonperfusion. Diabetic retinal vascular leakage, capillary nonperfusion, and endothelial cell damage are temporary and spatially associated with retinal leukocyte stasis in early experimental diabetes. Retinal leukostasis increases within days of developing diabetes and correlates with the increased expression of retinal intercellular adhesion molecule-1 (ICAM-1) and CD18. Mice deficient in the genes encoding for the leukocyte adhesion molecules CD18 and ICAM-1 were studied in two models of diabetic retinopathy with respect to the long-term development of retinal vascular lesions. CD18^{-/-} and ICAM-1^{-/-} mice demonstrate significantly fewer adherent leukocytes in the retinal vasculature at 11 and 15 months after induction of diabetes with STZ. This condition is associated with fewer damaged endothelial cells and lesser vascular leakage. Galactosemia of up to 24 months causes pericyte and endothelial cell loss and formation of acellular capillaries. These changes are significantly reduced in CD18- and ICAM-1-deficient mice. Basement membrane thickening of the retinal vessels is increased in long-term galactosemic animals independent of the genetic strain. Here we show that chronic, low-grade subclinical inflammation is responsible for many of the signature vascular lesions of diabetic retinopathy. These data highlight the central and causal role of adherent leukocytes in the pathogenesis of diabetic retinopathy. They also underscore the potential utility of anti-inflammatory treatment in diabetic retinopathy.

Key words: adhesion molecules • retina • vascular lesions

Despite current treatments and existing knowledge, diabetic retinopathy remains to be a major cause of blindness in patients aged 20–64 years. New evidence indicates that diabetic retinopathy may be an inflammatory disease. The retinal vasculature of diabetic humans contains increased numbers of leukocytes, a finding that coincides with the increased expression of ICAM-1 in retinal vasculature (1). The phenomenon is also present in diabetic animal models and occurs whether the diabetes is spontaneous in nature or is induced (2–4). The increased density of leukocytes in the retinal vasculature begins as early as 1 week following the onset of experimental diabetes and results in injury to the endothelium via a FasL-mediated mechanism; a process that leads to breakdown of the blood-retinal barrier (5–6). Blood-retinal barrier breakdown develops early in the course of diabetic retinopathy in humans and, as a long-term lesion is the major pathology leading to macular edema and the risk of subsequent visual loss.

Retinal ischemia is a second sight-threatening diabetic complication. Histopathological analyses have shown that areas of angiographic non-perfusion *in vivo* frequently co-localize to regions full of acellular capillaries, that is, basement membrane tubes devoid any viable endothelial cells or pericytes (7). These acellular capillaries are a hallmark of advanced human diabetic retinopathy and also develop in animal models of diabetes. Retinal ischemia is a direct consequence of acellular capillary formation and leads to the increased expression of vascular endothelial growth factor (VEGF). When VEGF levels in the retina and vitreous reach a certain threshold, pathological neovascularization of the retina, optic nerve, and iris ensue (8). The consequences of neovascularization are often severe, with vision loss resulting from bleeding, retinal detachment, and/or glaucoma. Pericyte and endothelial cell injury and death, the processes leading to acellular capillary formation, are now known to begin well before any clinical evidence of diabetic retinopathy is detected (5–9).

The leukocytes that adhere to the diabetic retinal vasculature use specific adhesion molecules such as the integrin ligand CD18, which forms the invariable portion of the heterodimers Mac-1 (CD11a/CD18) and LFA-1 (CD11b/CD18) (10). Leukocytes use CD18 to tether themselves to intercellular adhesion molecule-1 (ICAM-1) on the surface of diabetic retinal vasculature. Previous work has established the role of CD18/ICAM-1 leukocyte adhesion in the pathogenesis of early diabetes-induced leukostasis and blood-retinal barrier breakdown (5). However, the effect of chronic CD18 and ICAM-1-mediated leukocyte adhesion on the long-term functional and anatomic pathology of diabetic retinopathy has to date remained unknown. To address this issue we studied the incidence of the signature pathologies of diabetic retinopathy (leukostasis, vascular leakage, and histologic changes) in mice deficient in the ICAM-1 (11) and CD18 (12) genes in two established models of chronic diabetic retinopathy.

MATERIALS AND METHODS

Models of long-term diabetes

Male CD 18-deficient mice (C57BL/6J-*Itgb2*tm1bay), ICAM-1-deficient mice (C57BL/6J-*Icam1*tm1Bay), and normal male C57BL/6J mice, which served as controls, were purchased from Jackson Labs (Bar Harbor, ME) (11–12). Two models of long-term diabetes were used. One group had diabetes-induced via streptozotocin and was maintained in a diabetic state for 11 months. The second group was fed a high-galactose diet, a process that results in hyperglycemia

largely devoid the attendant metabolic abnormalities associated with diabetes. The latter model develops most of the classic histopathological lesions of diabetic retinopathy but is associated with less mortality than diabetes per se (13–14).

Following 8 h of fasting, mice weighing 18–25 g (Charles River, MA) received daily 60 mg/kg intraperitoneal injections of streptozotocin (Sigma, St. Louis, MO) in 0.05 M citrate buffer (pH 4.5) for 5 days. Control non-diabetic mice received citrate buffer alone. Animals with blood glucose levels above 250 mg/dl, 48 h following streptozotocin injection, were deemed diabetic. Prior to each experiment and sacrifice, the diabetic state was reconfirmed. The mice were fed standard laboratory chow and were allowed free access to food and water in an air-conditioned room with a 12 h light/12 h dark cycle. Experimental galactosemia was induced by feeding a diet of Teklad 7004 (Harlan, WI) enriched with 30% D-galactose. In all animals, body weight was measured weekly and blood hexose elevation was estimated by measuring the levels of nonenzymatic glycosylated hemoglobine (GHb; Glyc-Affin, Pierce, Rockford, IL). Animals with a GHb below the twofold of the normal value were excluded from the experiments.

Ex vivo retinal leukostasis quantitation

Quantification of retinal leukostasis was performed as described previously. Following the induction of deep anesthesia, the chest cavity was opened and a 22-gauge perfusion canula was introduced into the left ventricle. Drainage was achieved using a 16-gauge needle placed in the right atrium. Following perfusion with phosphate buffered saline (PBS) under physiological pressure (the bottle is adjusted at ~50 cm allowing for the heart to pump the fluid by its own force) to remove erythrocytes and non-adherent leukocytes, fixation with 1% paraformaldehyde was achieved. Non-specific binding was blocked with 1% albumin in PBS followed by perfusion with fluorescein-isothiocyanate (FITC)-coupled *Concanavalin A* lectin (20 µg/ml in PBS, pH 7.4; 5 mg/kg BW; Vector Labs, Burlingame, CA). *Concanavalin A* was used to label adherent leukocytes and vascular endothelial cells. Residual unbound lectin was removed with a 1% albumin in PBS perfusion for 1 min followed by a PBS perfusion for 4 min. The retinæ were carefully removed, and flat mounts were prepared by using a fluorescence anti-fading medium (Southern Biotechnology, Birmingham, AL). The retinæ were then imaged by using a fluorescence microscope (Zeiss Axiovert, Oberkochen, Germany, FITC filter). Retinæ in which the peripheral collecting vessels of the ora serrata were not visible were discarded. The total number of leukocytes in the retinal arterioles, venules, and capillaries was then determined.

Propidium iodide labeling

Dead and injured endothelial cells were labeled in vivo using propidium iodide (PI; Molecular Probes, Eugene, OR). Following the induction of deep anesthesia with 50 mg/kg IP sodium pentobarbital, PI (1 mg/ml in PBS) was injected intravenously via the tail vein at a concentration of 5 µmol/kg (0.668 ml/200 mg BW). The solution was allowed to circulate for 20 min, after which it was followed by body perfusion, fixation, and lectin labeling as described above. Retinal flat mounts were examined via fluorescence microscopy as described above. Labeled endothelial cells were distinguished from surrounding cells, especially pericytes, by focusing through the tissue to discern the distinct cellular outline and nuclear shape of the endothelial cells.

Measurement of retinal blood vessel leakage using Evans blue

Retinal blood vessel leakage was quantitated using Evans blue dye, which non-covalently binds to plasma albumin in the blood stream (15). Evans blue dye (Sigma) was prepared by dissolving it in normal saline (30 mg/ml), sonicating it for 5 min, and filtering it through a 5 µm filter. Under deep anesthesia, Evans blue was injected through the tail vein at a dose of 30 mg/kg. After the dye circulated for 60 min, the chest cavity was opened and the left heart ventricle was cannulated. Each mouse was perfused with citrate-buffered 1% paraformaldehyde (37°C) for 2 min to clear the dye, keeping the physiological pressure of 100 mm Hg. Immediately following perfusion, the eyes were enucleated and the retinæ were carefully dissected away under an operating microscope. The weight of each retina was measured after thorough drying in a Speed-Vac. Albumin leakage into the retinal tissue was estimated via the measurement of extravasated Evans blue dye. Evans blue was extracted by incubating each retina in 60 µl formamide for 18 h at 70°C. The extract was ultra-centrifuged at a speed of 70,000 rpm for 45 min at a temperature of 4°C. The absorbance of the supernatant was measured with a spectrophotometer at 620 nm, the absorption maximum for Evans blue in formamide. The concentration of dye in the extracts was calculated from a standard curve of Evans blue in formamide and normalized to the dry retinal weight (15).

Trypsin digest procedure

Trypsin digestion of the retina was performed according to the method of Cogan et al. (16) with some modifications (17). The digestion buffer contained 0.2 M sodium fluoride to inhibit DNases contaminating the crude trypsin preparation. Four to five retinæ per group were analyzed. A masked observer performed all measurements, which entailed a quantitative measure of the cells of interest in four standardized high-power fields per quadrant.

Electron microscopy

For the electron microscopy analyses of the retinas, enucleated eyes were fixed overnight at 4°C in 4% glutaraldehyde and processed as described previously (17). Electron micrographs of the retinal capillaries were obtained at 20,000 × magnification. Each one eye of a mouse was used for electron microscopy, whereas the other one was processed for trypsin digestion. From each eye five representative sections were selected, and five vessels per retina were analyzed. The thickness of basement membranes, measured in retinal capillaries with a diameter of less than 1000 nm on photo prints, was calculated for each vessel. Each three measurements per vessels were included into the calculation to account for variations in BM thickness exists around the capillaries at pericyte, glia, and endothelial cell interfaces. ([Table 3](#)).

Statistics

Statistical analysis was performed by using a non-parametric Kruskal-Wallis test followed by Fisher's multiple comparison test. ANOVA (ANOVA) followed by Fisher's multiple comparison tests yielded similar conclusions. Differences were considered statistically significant when the *P* values were less than 0.05.

RESULTS

Blood glucose levels in the two groups of long-term diabetic mice

Throughout all facets of the study, the animals in both groups exhibited systemic elevation of their blood hexose levels ([Tables 1, 2](#)). As expected, mortality in the STZ-diabetic group increased significantly after 12 months of diabetes, precluding further investigation beyond that time point. However, the galactose-fed hyperglycemic mice were relatively long-lived and were used to assess retinopathy beyond the one-year time point.

CD18 and ICAM knockout mice exhibit decreased leukostasis in two models of long-term diabetes

Adherent leukocytes were quantified in the retinal vasculature following in situ labeling with *Concanavalin A* (5). All non-adherent blood elements were removed via whole body perfusion at a physiological pressure. Retinal flat mounts were prepared, and the adherent leukocytes were counted in the whole retina. Leukocyte adhesion was suppressed in the ICAM-1^{-/-} and CD18^{-/-} mice after 11 months of diabetes. The retinas of the wild-type mice showed a 3.1-fold increase in the number adherent leukocytes compared with the age-matched non-diabetic controls ($n=12$, 23.1 ± 5.8 vs. 7.5 ± 3.5 adherent leukocytes per retina; $P<0.0001$). In contrast, the number of adherent leukocytes in the 11-month diabetic CD18^{-/-} mice ($n=12$, 7.72 ± 3.43 leukocytes per retina) and ICAM-1^{-/-} mice ($n=12$, 6.8 ± 3.8 leukocytes per retina) did not significantly differ from the non-diabetic wild-type mice ($P>0.05$ for both). For both the CD18^{-/-} and ICAM-1^{-/-} mice, the number of adherent leukocytes in non-diabetic animals was slightly lower than in non-diabetic wild-type controls ($n=12$, 4.4 ± 2.7 , and 5.6 ± 4.6 leukocytes per retina, respectively; $P>0.05$ for both) ([Fig. 1A](#)).

CD18 and ICAM knockout mice bear decreased numbers of injured endothelial cells in two models of long-term diabetes

Endothelial cell injury was assessed with propidium iodide (PI), a fluorophore that is excluded from uninjured cells but whose uptake is diagnostic for injured and/or dying cells (5). Propidium iodide labeling revealed little or no labeling in the non-diabetic retinae ($n=12$, 1.6 ± 2.4 PI positive cells per retina; $P>0.05$). In contrast, endothelial labeling was markedly increased in the retinae of the 11-month diabetic mice ($n=12$, 32.5 ± 13.9 PI positive cells per retina; $P<0.0001$; [Fig. 1A](#)). However, propidium iodide labeling was potently reduced in the diabetic CD18^{-/-} and ICAM-1^{-/-} mice ($n=12$, 0.7 ± 0.9 , and 1.5 ± 1.7 positive cells per retina respectively; $P<0.0001$ vs. diabetic wild-type controls; [Fig. 1A](#)).

CD18 and ICAM knockout mice exhibit decreased blood-retinal barrier breakdown in two models of long-term diabetes

Evans-blue can be used to quantitatively assess subtle degrees of blood-retinal barrier breakdown (mean \pm SE μl plasma \times g retinal dry weight⁻¹ \times h⁻¹) (15). In the 11-month diabetic wild-type mice, blood-retinal barrier breakdown was increased when compared with non-diabetic age-matched controls (8.3 ± 0.5 vs. 0.3 ± 0.1 , $n=7$; $P<0.0005$). However, blood-retinal barrier breakdown was markedly inhibited in the diabetic CD18^{-/-} (0.8 ± 0.2 vs. 0.5 ± 0.1 , $n=7$; $P<0.01$)

and ICAM-1^{-/-} mice ($n=6$, 1.1 ± 0.3 vs. 0.4 ± 0.1 ; $P<0.01$) mice. Thus, diabetic CD18^{-/-} and ICAM-1^{-/-} mice manifested 90 and 87% less blood-retinal barrier breakdown, respectively, than the wild-type age-matched diabetic mice ([Fig. 1B](#)).

CD18 and ICAM knockout mice exhibit less severe histopathological changes after 11 month of diabetes

In addition to its functional vascular abnormalities, diabetic retinopathy is also defined by its unique vascular histopathology. Retinal vascular lesions were assessed via trypsin digestion, a method that permits detailed analysis of the retinal vascular anatomy in isolation (16–17).

Endothelial cells form the monolayers that line the intraluminal surface of viable capillaries. In the 11-month wild-type diabetic mice, the number of endothelial cells was reduced by 29% ($n=5$, 59.8 ± 4.1 vs. 78.4 ± 15.5 ; $P<0.05$ vs. the non-diabetic controls; $P<0.005$ vs. age-matched non-diabetic wild-type controls; [Fig. 2A](#)). In contrast, the endothelial cell counts in the ICAM-1^{-/-} and CD18^{-/-} mice were normal ($n=5$, 85.8 ± 3.2 vs. 90 ± 50.4 and 71.8 ± 9.0 vs. 83.4 ± 17.53 , respectively; $P > 0.05$ for both vs. non-diabetic controls; $P > 0.05$ vs. non-diabetic wild-type mice; [Fig. 2A](#)).

The appearance of pericyte “ghosts”, that is, dead pericytes, is a signature lesion of diabetic retinopathy. The number of pericytes was reduced by 40.9% in the 11-month diabetic wild-type mice ($n=5$, 20.2 ± 3.4 vs. 34.2 ± 9.6 ; $P<0.0001$). However, no significant reduction was seen in the 11-month diabetic ICAM-1^{-/-} and CD18^{-/-} mice when compared with their non-diabetic controls ($n=5$, 35.2 ± 7.6 vs. 35.8 ± 4.8 and 24.6 ± 4.3 vs. 29.4 ± 5.6 respectively; $P>0.05$ for each). In the CD18- and ICAM-1-deficient mice, the diabetes-induced increases in pericyte death were suppressed by 55 and 66% respectively, ($P<0.0001$ vs. age-matched 11 month-diabetic wild-type mice). In agreement with this finding, the number of normal appearing pericytes in the diabetic ICAM-1^{-/-} and CD18^{-/-} mice was significantly greater than in the age-matched diabetic wild-type controls ($P<0.05$, [Fig. 2B](#)) and did not differ significantly from that of the age-matched non-diabetic wild-type controls.

In the 11-month diabetic wild-type mice, the number of acellular capillaries increased 3.8-fold compared with the non-diabetic wild-type controls ($n=5$, 12.5 ± 2.6 vs. 3.2 ± 0.5 ; $P<0.0001$), a pathology that was suppressed by 60 and 56% in the diabetic CD18^{-/-} and ICAM-1^{-/-} mice, respectively ($P<0.0001$ vs. age-matched diabetic wild-type mice): no increase in acellular capillaries was observed in either the ICAM-1^{-/-} and CD18^{-/-} mice ($n=5$, 4.3 ± 2.6 vs. 5.3 ± 1.0 , and 5.6 ± 1.8 vs. 4.3 ± 1.3 , respectively; $P>0.05$ for each; [Fig. 2C](#)).

CD18 and ICAM knockout mice show less severe histopathological changes in a model of long-term diabetes

ICAM-1 or CD18 deficiency also inhibited the development of more advanced retinopathy in the galactosemic mice. These animals were galactosemic for up 24 months, almost the entire normal murine lifespan. As was observed in the diabetic mice, galactosemia caused both the number of endothelial cells and pericytes to decrease over time in the wild-type animals ([Fig. 3](#)). After 22 months of galactosemia, the number of endothelial cells decreased 25% in the wild-type mice compared with the age-matched euglycemic wild-type controls (58.3 ± 26.07 vs. 78.4 ± 15.6 ,

$n=4$, $P<0.005$). In contrast the 22-month galactosemic ICAM-1^{-/-} and CD18^{-/-} mice were largely protected against this loss. Compared with the age-matched normal controls, the endothelial cell counts were reduced by only 19% ($P<0.001$) in the galactosemic ICAM-1^{-/-} mice. ICAM-1^{-/-} mice exhibited 77.7 ± 15.1 endothelial cells/field after 22 months of galactose feeding as compared with 90 ± 15.4 cells in ICAM-1^{-/-} mice fed with normal chow ($n=4$; $P>0.05$). Endothelial cell counts were essentially normal in the CD18^{-/-} mice ($n=4$, 82.4 ± 10.6 vs. 83.4 ± 17.5 ; $P>0.05$; [Fig. 3A](#)). After 22 months, the number of pericytes was decreased 55% in the galactosemic wild-type mice (15.2 ± 6.01 pericytes per field as compared with 34.2 ± 9.6 in the age-matched wild-type non-galactosemic mice ($n=4$; $P<0.002$; [Fig. 3B](#)). In contrast, no significant decrease in pericytes was observed in the 22-month ICAM-1^{-/-} ($n=4$, 28.8 ± 5.2 vs. 35.8 ± 4.8 ; $P>0.05$) or CD18^{-/-} (30.2 ± 5.0 vs. 29.4 ± 5.6 ; $n=4$; $P>0.05$) galactosemic mice ($P>0.05$ vs. euglycemic wild-type controls).

The formation of acellular capillaries was quantified as described previously (14). In all non-diabetic and non-galactosemic groups, 5 or fewer acellular capillaries per retina were found at 24 months (wild-type: 3.3 ± 0.5 ; ICAM-1^{-/-}: 5.3 ± 1.0 ; CD18^{-/-}: 4.3 ± 1.3). The acellular capillary data in the galactosemic mice closely mirrored those of the diabetic mice ([Fig. 3C](#)). For the wild-type C57/BL6 mice, 22 months of galactosemia resulted in an eightfold increase to 26.3 ± 6.6 acellular in acellular capillaries ($n=4$; $P<0.0001$). In contrast, the 22-month galactosemic ICAM-1^{-/-} and CD-18^{-/-} mice developed 56 and 60% fewer acellular capillaries, respectively [ICAM-1^{-/-} mice had 11.5 ± 7.8 acellular capillaries, similar to CD18^{-/-} mice, which showed 10.5 ± 3.3 acellular capillaries ($P<0.005$ for each)]. [Fig. 3D](#) shows representative trypsin digests from each treatment group.

Basement membrane thickening is a consistent feature in human diabetic retinopathy and similarly develops in the diabetic and galactosemic animal models. As expected, established ultrastructural methods (17) demonstrated a thickening of the capillary basement membrane in both the diabetic and galactosemic cohorts. However, surprisingly no suppression of basement membrane thickening in the ICAM-1^{-/-} and CD 18^{-/-} deficient mice was apparent ($P>0.05$ for both vs. wild-type controls; data not shown), which suggests an alternative mechanism of causation ([Table 3](#)).

DISCUSSION

Taken together, these data demonstrate that the reduced expression of ICAM-1, or its leukocyte counter-receptor, CD18, significantly inhibits the formation of acellular capillaries in experimental models of diabetic retinopathy. Previous work has demonstrated that adherent leukocytes can mediate endothelial cell and vascular leakage (4, 5). However, the primacy of leukocytes in the long-term development of diabetic retinal endothelial cell death is in doubt. To address this issue, we used a long-term mouse model of diabetic retinopathy. Our model of STZ-induced diabetes was limited to a duration of 15-month diabetes, as the death rate increased significantly thereafter and the required numbers of animals could not be maintained. Interestingly, diabetic mice did not drop in weight or die by direct consequences of diabetes such as hypo- or hyperglycemia but died of STZ-associated tumors as previously reported by others (18, 19). However, even after 11 months of STZ-induced diabetes, functional as well as histopathological changes were apparent. Galactose feeding, however, allowed for analysis of the

histopathological alterations as long as 24 month. Previous studies using a galactose-induced retinopathy had demonstrated the formation of acellular capillaries, pericyte and endothelial cell loss, and microaneurysm formation (14). We assume that the current findings are relevant to human diabetes because rodent and human diabetes share many features: histopathological alterations, blood-retinal barrier breakdown, leukocyte buildup, and ICAM-1 up-regulation.

Leukocyte adhesion to the diabetic vascular endothelium can promote receptor-mediated endothelial apoptosis via a Fas/FasL mechanism in a short-term model of diabetic retinopathy (6). The reduction in acellular capillaries in the diabetic ICAM^{-/-} and CD18^{-/-} mice is a direct measure of the protective effect of inflammation suppression has on cell death in the vasculature.

Surprisingly, the inhibition of leukocyte adhesion also prevented the loss of pericytes, which are not typically in direct contact with adherent leukocytes in the vasculature. Interestingly, our data confirm the pericyte loss as one of the first histopathological features of diabetic retinopathy. Compared with o endothelial cells, which are reduced by half after 24 month of diabetes, only one-third of the number of pericytes remains. This finding can explain the widespread idea that pericyte loss is one of the earliest changes in the diabetic retina. However, our current and previous data demonstrate that alterations in the leukocyte-endothelial interaction might occur far before and are yet responsible for the pericyte damage (5), as inhibition of the leukocyte-endothelial interaction can prevent, at least in part, the pericyte loss. Similar to the recent findings on the role of the angiopoietins in inflammation, which were first known to affect the pericyte-endothelial interactions (20), the current data suggest that the mechanisms involved in the cellular interactions in diabetes are more complex than currently accepted.

We hypothesize here, as others have before us (21, 22), that acellular capillaries are the eventual product of chronic, repetitive, leukocyte-mediated injury to the vasculature. The damage begins early in diabetes; with time, parts of the vasculature become irreparable as the vascular cells reach replicative senescence.

The long-term wild-type diabetic animals in the current study also manifested blood-retinal barrier breakdown, one of the most important functional pathologies in diabetic retinopathy. Blood-retinal barrier breakdown was almost totally suppressed in the long-term diabetic ICAM-1^{-/-} and CD18^{-/-} animals. Many mechanisms may be responsible for this effect and include: (i) direct leukocyte-mediated endothelial cell injury and death; (ii) leukocyte-mediated injury of the supportive cells, e.g., pericytes; (iii) leukocyte-induced opening of tight junctions; and (iv) release of permeability factors such as VEGF from leukocytes, which can directly affect the tight junctions and fenestrae of the endothelial barrier.

The inhibition of the anatomic vascular pathologies associated with diabetes was not total in the ICAM-1^{-/-} and CD18^{-/-} animals. One potential reason is that the mice used in these experiments possessed hypomorphic rather than null alleles for CD18 and ICAM-1 (11). In the case of the CD18-deficient mice, the homozygous mutants retain between 2 and 16% of normal granulocyte CD18 expression, the exact amount depending on the state of granulocyte activation (12). The lack of complete protection against the histopathological changes of diabetic retinopathy may be attributed to this residual expression. Alternatively, the lack of complete suppression may indicate that alternative pathways are operative in the generation of diabetic retinopathy.

It can be assumed that different molecules are involved in the stepwise process of leukocyte-endothelial interaction in diabetes and that these molecules are differentially expressed during the course of the disease. Selectin levels were found to be highest in patients with severe non-proliferative diabetic retinopathy in contrast to sVCAM-1 levels, which were highest in patients with proliferative diabetic retinopathy (23–25). The selectins, which mediate leukocyte-rolling rather than sticking, however, have not been found to be directly involved in leukocyte-mediated endothelial apoptosis or damage “in vivo” (Joussen et al., unpublished). Interestingly, other mediators are involved in the concert of factors that mediate diabetic leukocyte adhesion. We had previously found that angiopoietin-1 can inhibit diabetes induced leukostasis in a rat model (26). Angiopoietin-1 counteracts the VEGF-induced inflammation by reducing VEGF-induced endothelial adhesiveness (20) and might thus be involved in the altered expression of adhesion molecules.

Notably, one important histopathological change that was not prevented was thickening of the capillary basement membrane, which suggests that the process is independent of leukocyte adhesion. Biochemical changes unrelated to the leukocyte injury, e.g., aldose reductase activation, may contribute independently to the production of a thickened vascular basement membrane.

In conclusion, these data demonstrate that ICAM-1- and CD18-mediated leukocyte adhesion is increased in the retinal vasculature of mice with long-term diabetes or experimental elevation of blood hexose (galactosemia) and accounts for many of the signature lesions of diabetic retinopathy. These data also identify ICAM-1 and CD18 as potential therapeutic targets, which in combination with adequate glycemic control may be used to manage the vision-threatening sequelae of diabetes.

ACKNOWLEDGMENTS

We thank the Roberta W. Siegel Fund (A.P.A.); the Juvenile Diabetes Foundation International (A.M.J. and A.P.A.); Deutsche Forschungsgemeinschaft DFG Jo 324 / 2-1, DFG Jo 324/ 4-1 and, DFG Jo 324/ 6-1, Jo 324/ 6-2 (Emmy-Noether) (A.M.J.); the Ernst- und Berta Grimmke Stiftung, Düsseldorf (A.M.J.); the Meyer-Schwarting Stiftung, Bremen (A.M.J.); the Kämpgen Stiftung, Köln (A.M.J. and B.K.); the Werner und Gertrud Müller Stiftung (A.M.J.); Iacocca Foundation and Falk Foundation (A.P.A.) and NIH EY11627 and EY12611 (A.P.A.) for their support.

REFERENCES

1. McLeod, D. S., Lefer, D. J., Merges, C., and Luty, G. A. (1995) Enhanced expression of intracellular adhesion molecule-1 and P-selectin in the diabetic human retina and choroid. *Am. J. Pathol.* **147**, 642–653
2. Schröder, S., Palinski, W., and Schmid-Schönbein, G. W. (1991) Activated monocytes and granulocytes, capillary nonperfusion, and neovascularization in diabetic retinopathy. *Am. J. Pathol.* **139**, 81–100
3. Miyamoto, K., Hiroshiba, N., Tsujikawa, A., and Ogura, Y. (1998) In vivo demonstration of increased leukocyte entrapment in retinal microcirculation of diabetic rats. *Invest. Ophthalmol. Vis. Sci.* **39**, 2190–2194

4. Miyamoto, K., et al. (1999) Prevention of leukostasis and vascular leakage in streptozotocin-induced diabetic retinopathy via intercellular adhesion molecule-1 inhibition. *Proc. Natl. Acad. Sci. USA.* **96**, 10836–10841
5. Jousseaume, A. M., et al. (2001) Leukocyte-mediated endothelial cell injury and death in the diabetic retina. *Am. J. Pathol.* **158**, 147–152
6. Jousseaume, A. M., et al. (2003) Suppression of Fas-FasL-induced endothelial cell apoptosis prevents diabetic blood-retinal barrier breakdown in a model of streptozotocin-induced diabetes. *FASEB J.* **17**, 76–78
7. Kohner, E. M., and Henkind, P. (1970) Correlation of fluorescein angiogram and retinal digest in diabetic retinopathy. *Am. J. Ophthalmol.* **69**, 403–414
8. Miller, J. W., et al. (1994) Vascular endothelial growth factor/vascular permeability factor is temporally and spatially correlated with ocular angiogenesis in a primate model. *Am. J. Pathol.* **145**, 574–584
9. Mizutani, M., Kern, T. S., and Lorenzi, M. (1996) Accelerated death of retinal microvascular cells in human and experimental diabetic retinopathy. *J. Clin. Invest.* **97**, 2883–2890
10. Barouch, F. C., et al. (2000) Integrin-mediated neutrophil adhesion and retinal leukostasis in diabetes. *Invest. Ophthalmol. Vis. Sci.* **41**, 1153–1158
11. Sligh, J. E., Jr., et al. (1993) Inflammatory and immune responses are impaired in mice deficient in intercellular adhesion molecule 1. *Proc. Natl. Acad. Sci. USA.* **90**, 8529–8533
12. Wilson, R. W., et al. (1993) Gene targeting yields a CD18-mutant mouse for study of inflammation. *J. Immunol.* **151**, 1571–1578
13. Kern, T. S., and Engerman, R. L. (1995) Galactose-induced retinal microangiopathy in rats. *Invest. Ophthalmol. Vis. Sci.* **36**, 490–496
14. Kern, T. S., and Engerman, R. L. (1996) A mouse model of diabetic retinopathy. *Arch. Ophthalmol.* **114**, 986–990
15. Xu, Q., Qaum, T., and Adamis, A. P. (2001) Sensitive blood-retinal barrier breakdown quantitation using Evans blue. *Invest. Ophthalmol. Vis. Sci.* **42**, 789–794
16. Cogan, D. G., Toussaint, D., and Kuwabara, T. (1961) Retinal vascular patterns. IV. Diabetic retinopathy. *Arch. Ophthalmol.* **66**, 366–378
17. Kern, T. S. and Engerman, R. L. Vascular lesions in diabetes are distributed non-uniformly within the retina. *Exp. Eye. Res.* **60**, 545–549

18. Chieco, P., Venturini, A. P., Barbanti, M., and Romagnoli, E. (1993) A quantitative cytochemical study on the pathogenesis of streptozotocin-induced epithelial tumors in rat kidney. *Toxicol. Pathol.* **21**, 402–408
19. Cutler, L. S., Pinney, H. E., Christian, C., and Russotto, S. B. (1979) Ultrastructural studies of the rat submandibular gland in streptozotocin induced diabetes mellitus. *Virchows Arch. A Pathol. Anat. Histol.* **382**, 301–311
20. Kim, I., Moon, S. O., Park, S. K., Chae, S. W., and Koh, G. Y. (2001) Angiopoietin-1 reduces VEGF-stimulated leukocyte adhesion to endothelial cells by reducing ICAM-1, VCAM-1, and E-selectin expression. *Circ. Res.* **89**, 477–479
21. Bullard, S. R., Hatchell, D. L., Cohen, H. J., and Rao, K. M. (1994) Increased adhesion of neutrophils to retinal vascular endothelial cells exposed to hyperosmolarity. *Exp. Eye Res.* **58**, 641–647
22. Freedman, S. F., and Hatchell, D. L. (1992) Enhanced superoxide radical production by stimulated polymorphonuclear leukocytes in a cat model of diabetes. *Exp. Eye Res.* **55**, 767–773
23. Karadayi, K., Top, C., and Gulecek, O. (2003) The relationship between soluble L-selectin and the development of diabetic retinopathy. *Ocul. Immunol. Inflamm.* **11**, 123–129
24. Knudsen, S. T., Foss, C. H., Poulsen, P. L., Bek, T., Ledet, T., Mogensen, C. E., and Rasmussen, L. M. (2003) E-selectin-inducing activity in plasma from type 2 diabetic patients with maculopathy. *Am. J. Physiol. Endocrinol. Metab.* **284**, E1–E6
25. Limb, G. A., Hickman-Casey, J., Hollifield, R. D., and Chignell, A. H. (1999) Vascular adhesion molecules in vitreous from eyes with proliferative diabetic retinopathy. *Invest. Ophthalmol. Vis. Sci.* **40**, 2453–2457
26. Jousen, A. M., Poulaki, V., Tsujikawa, A., Qin, W., Qaum, T., Xu, Q., Moromizato, Y., Bursell, S. E., Wiegand, S. J., Rudge, J., et al. (2002) Suppression of diabetic retinopathy with angiopoietin-1. *Am. J. Pathol.* **160**, 1683–1693

Received January 5, 2004; accepted April 24, 2004.

Table 1**Mean blood sugar levels \pm standard deviation following STZ-induced diabetes.**

	C57/BL6 (wild-type)		ICAM-1^{-/-}		CD 18^{-/-}	
	Diabetic (mg/dl)	Non-Diabetic (mg/dl)	Diabetic (mg/dl)	Non-Diabetic (mg/dl)	Diabetic (mg/dl)	Non-Diabetic (mg/dl)
3 Weeks	445 \pm 49	103 \pm 16	472 \pm 69	137 \pm 36	416 \pm 79	137 \pm 75
6 Months	418 \pm 37	112 \pm 25	432 \pm 74	130 \pm 41	464 \pm 26	130 \pm 21
11 Months	434 \pm 74	112 \pm 30	423 \pm 71	134 \pm 28	401 \pm 114	101 \pm 10

P > 0.05 for variations among diabetic groups at all time points.

Table 2

Glycated hemoglobin levels in galactose-fed animals using affinity chromatography (Glyc-Affin, Pierce, Rockford, IL).

	C57/Bl6 (wild-type)	CD18^{-/-}	ICAM-1^{-/-}
Age-matched control	2.5 ± 0.7%	1.7 ± 0.5%	1.8 ± 0.4%
11 months galactosemia	7.1 ± 0.7%	7 ± 0.5%	7.4 ± 0.6%
16 months galactosemia	6.3 ± 0.6%	6.3 ± 0.3%	7.2 ± 0.3%
22 months galactosemia	6.8 ± 0.6%	6.3 ± 0.4%	7.1 ± 0.3%

P > 0.05 for variations among galactosemic groups at all time points.

Table 3**Basement membrane thickness of retinal capillaries (diameter < 1000 nm) in nm.**

	C57/Bl6 (wild-type)	CD18^{-/-}	ICAM-1^{-/-}
Age-matched control	5 ± 0.2	5.2 ± 0.9	4.7 ± 1.3
22 months galactosemia	9.3 ± 3.1	11.4 ± 4.8	9.5 ± 0.8

A mean value from three measurements was calculated for each vessel. Three vessels of three retinas were measured per condition. $P > 0.05$ for variations among galactosemic groups at all time points.

Fig. 1

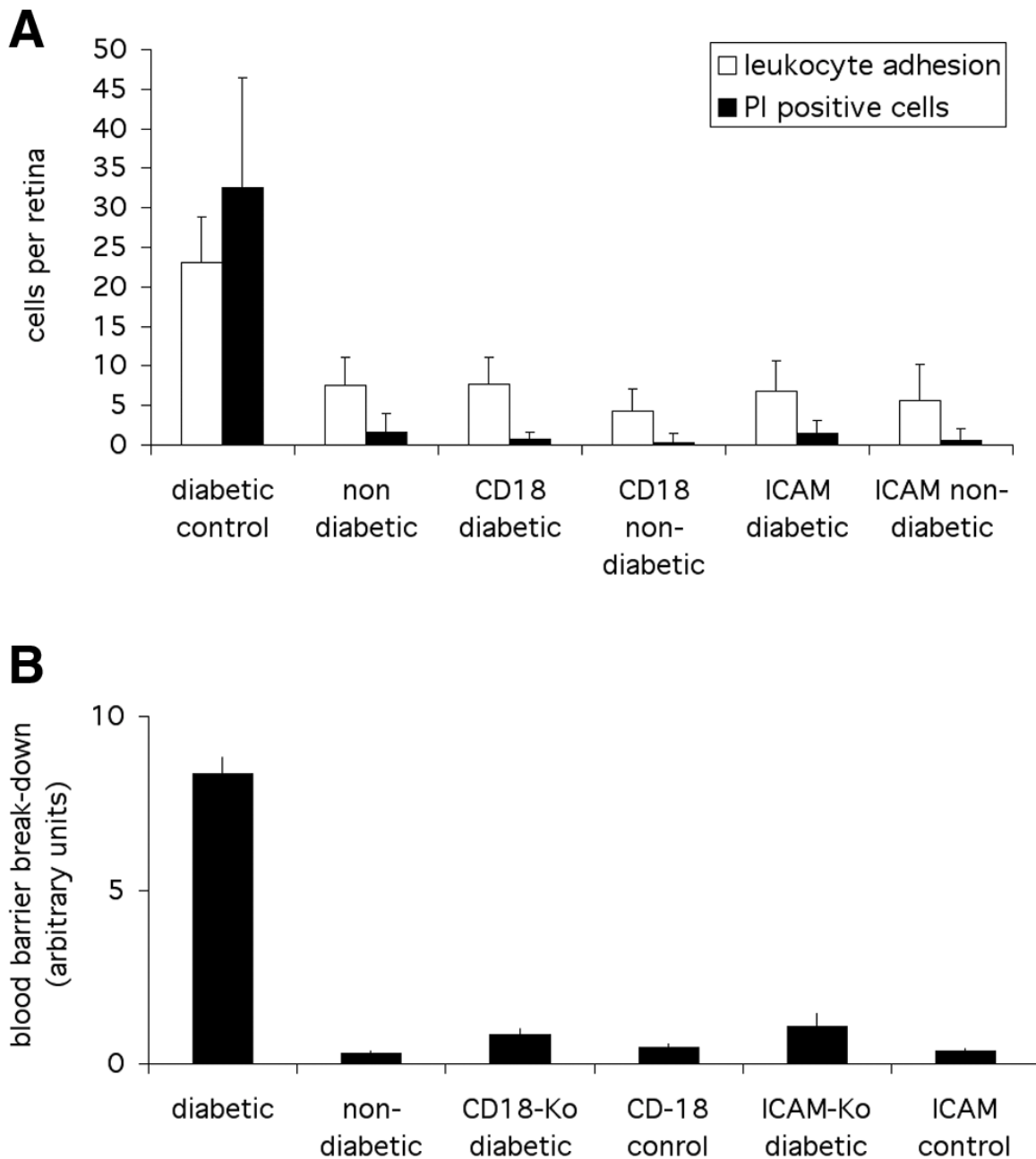


Figure 1. **A)** Adherent leukocytes were quantified in the retinal vasculature following in situ labeling with *Concanavalin A* (5). All non-adherent blood elements were removed via whole body perfusion at a physiological pressure. After 11 months of diabetes, the number of adherent leukocytes in the wild-type (C57BL/6J) mice was 3.7-fold greater than in the age-matched, non-diabetic, wild-type controls ($P < 0.001$). In contrast, the number of adherent leukocytes in the diabetic CD18^{-/-} or ICAM-1^{-/-} (C57BL/6J) mice did not differ significantly from that of the non-diabetic, wild-type controls or the non-diabetic CD18^{-/-} and ICAM-1^{-/-} age-matched controls ($P > 0.05$ for all). **B)** Endothelial cell injury was assessed with propidium iodide (PI), a fluorophore that is excluded from uninjured cells but whose uptake is diagnostic for injured and/or dying cells (5). Little or no endothelial injury was observed in the retinas of the non-diabetic, wild-type ICAM-1^{-/-} or CD18^{-/-} mice. However a marked increase in endothelial cell injury was detected in the retinal vessels of the 11-month diabetic, wild-type mice ($P < 0.001$). In contrast, the diabetic CD18^{-/-} and ICAM-1^{-/-} mice had markedly less endothelial cell injury ($P < 0.001$ vs. the age-matched wild-type diabetic mice).

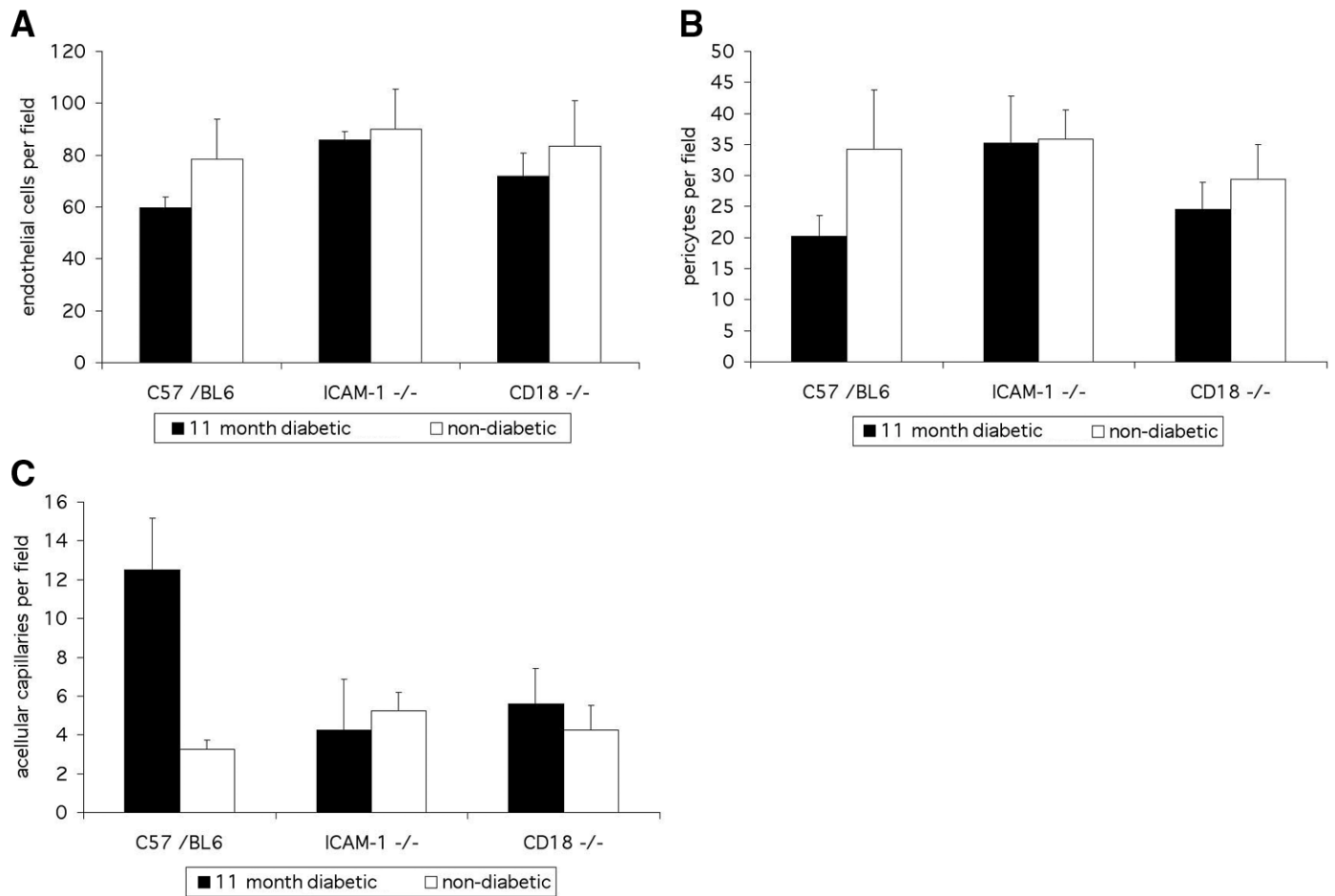
Fig. 2

Figure 2. In the 11-month, wild-type diabetic mice, the number of endothelial cells was reduced by 29% ($P < 0.005$ vs. age-matched non-diabetic, wild-type controls). In contrast, the endothelial cell counts in the ICAM-1^{-/-} and CD18^{-/-} mice were normal ($P > 0.05$ vs. non-diabetic wild-type mice; **A**). The appearance of pericyte “ghosts,” i.e., dead pericytes, is a signature lesion of diabetic retinopathy. In the CD18 and ICAM-1 deficient mice, the diabetes-induced increases in pericyte death were suppressed by 55 and 66%, respectively, ($P < 0.0001$ vs. age-matched, 11-month, diabetic wild-type mice). In agreement with this finding, the number of normal-appearing pericytes in the diabetic ICAM-1^{-/-} and CD18^{-/-} mice was significantly greater than in the age-matched, diabetic, wild-type controls ($P < 0.05$) and did not differ significantly from that of the age-matched, non-diabetic, wild-type controls (**B**). Following 11 months of diabetes, the retinas of the wild-type C57/B16 mice possessed 3.8-fold more acellular capillaries ($P < 0.001$; **Fig. 2C**), a pathology that was suppressed by 60 and 56% in the diabetic CD18^{-/-} and ICAM-1^{-/-} mice, respectively ($P < 0.0001$ vs. age-matched, diabetic, wild-type mice). In the non-diabetic animals, ICAM-1 or CD18 deficiency did not alter the number of acellular capillaries, which remained low as the animals aged ($P > 0.05$ vs. age-matched, wild-type controls; **C**).

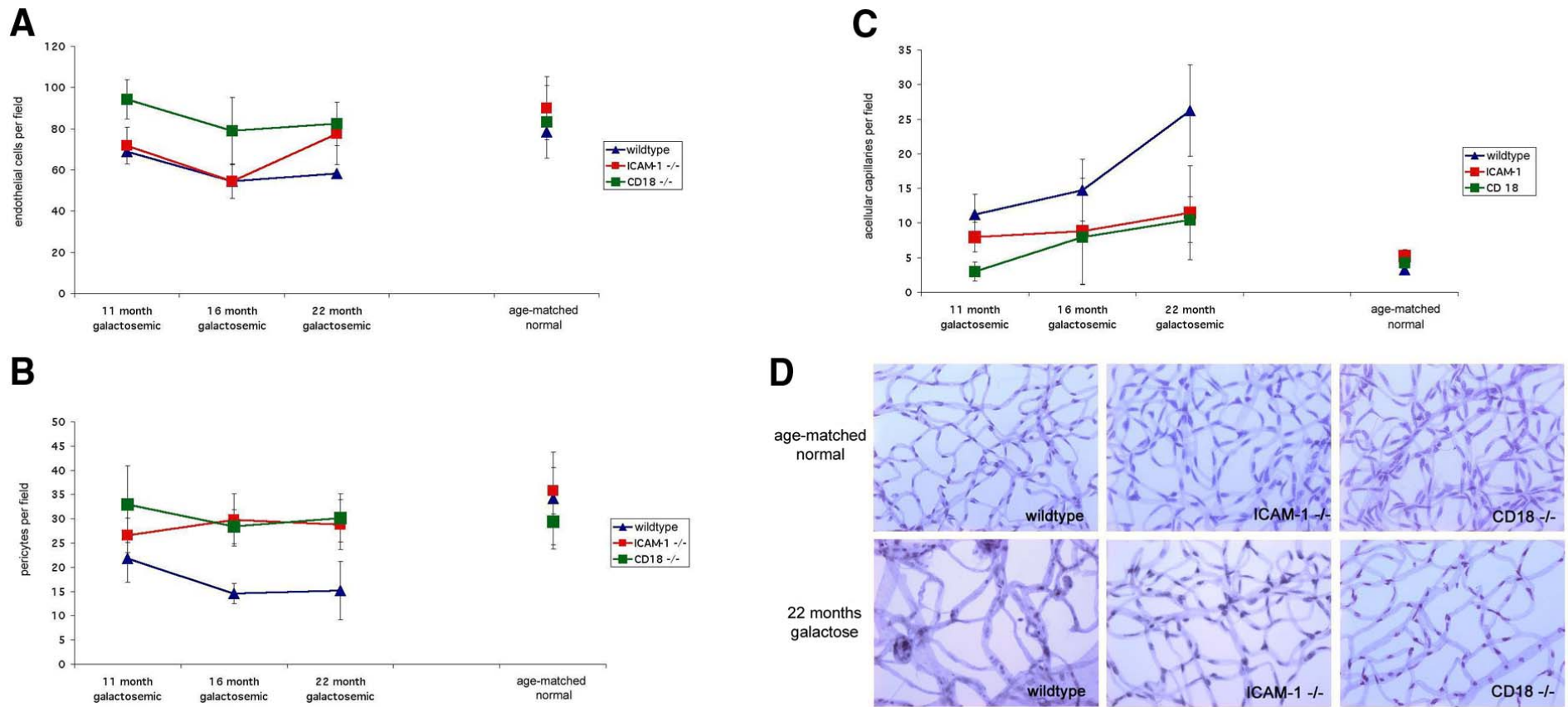
Fig. 3

Figure 3. Retinopathy was investigated in galactosemic ICAM-1^{-/-} and CD18^{-/-} mice as well as their respective wild-type controls. Both the number of endothelial cells and pericytes per field significantly decreased throughout the course of the disease in the wild-type, galactosemic animals (**A**, **B**). In the wild-type mice, the number of endothelial cells was decreased after 22 months of galactose feeding ($P < 0.05$). In contrast, the ICAM-1^{-/-} mice exhibited 77.7 ± 15.1 endothelial cells/field after 22 months of galactose feeding compared with 90 ± 15.4 cells in ICAM-1^{-/-} mice fed with normal chow ($P > 0.05$). The galactosemic CD18^{-/-} mice were similarly less prone to endothelial cell loss ($P > 0.05$; **A**). After 22 months of galactosemia, 15.2 ± 6.01 pericytes were found per field compared with 34.2 ± 9.6 in the age-matched, wild-type non-galactosemic mice ($P < 0.002$; **B**). In contrast, no significant decrease in pericytes was observed in the CD18^{-/-} mice ($P > 0.05$). Similarly, the ICAM-1^{-/-} mice demonstrated no significant decrease in pericyte counts after 22 months of galactose feeding compared with age-matched ICAM-1^{-/-} mice fed normal lab chow ($P > 0.05$). The formation of acellular capillaries was quantified as described previously (17). In all non-diabetic and non-galactosemic groups, 5 or fewer acellular capillaries per retina were found at 24 months. In the galactosemic wild-type mice, the number of acellular capillaries increased with the increasing duration of galactose feeding. After 24 months of galactosemia, an almost eightfold increase was found in the wild-type C57/BL6 mice ($P < 0.0001$; **C**). In contrast, after 22 months of galactose feeding, the ICAM-1^{-/-} mice had 11.5 ± 7.8 acellular capillaries, similar to CD18^{-/-} mice, which showed 10.5 ± 3.3 acellular capillaries ($P < 0.005$ for each). Representative images of the capillary bed are shown in (**D**).